Progression of Osteogenic Cell Cultures Grown on Microtopographic Titanium Coated With Calcium Phosphate and Functionalized With a Type I Collagen-Derived Peptide

Karina K.Y. Pereira,* Olívia C. Alves,* Arthur B. Novaes Jr.,* Fabíola S. de Oliveira,* Ji-Hyun Yi,† Osvaldo Zaniquelli,* Cornelia Wolf-Brandstetter,‡ Dieter Scharnweber,‡ Fabio Variola,§ Antonio Nanci,† Adalberto L. Rosa,* and Paulo T. de Oliveira*

Background: The functionalization of metallic surfaces aims at promoting the cellular response at the biomaterial–tissue interface. This study investigates the effects of the functionalization of titanium (Ti) microtopography with a calcium phosphate (CaP) coating with and without peptide 15 (P-15), a synthetic peptide analog of the cell-binding domain of collagen I, on the in vitro progression of osteogenic cells.

Methods: Sandblasting and acid etching (SBAE; control) Ti microtopography was coated with CaP, enabling the loading of two concentrations of P-15: 20 or 200 μg/mL. A machined Ti was also examined. Rat calvarial osteogenic cells were cultured on Ti disks with the surfaces mentioned above for periods up to 21 days (n = 180 per group).

Results: CaP coating exhibited a submicron-scale needle-shaped structure. Although all surfaces were hydrophobic at time zero, functionalization increased hydrophilicity at equilibrium. Microtopographies exhibited a lower proportion of well-spread cells at 4 hours of culture and cells with long cytoplasmic extensions at day 3; modified SBAE supported higher cell viability and larger extracellular osteopontin (OPN) accumulation. For SBAE and modified SBAE, real-time polymerase chain reaction showed the following results: 1) lower levels for runt-related transcription factor 2 at 7 days and for bone sialoprotein at days 7 and 10 as well as higher OPN levels at days 7 and 10 compared to machined Ti; and 2) higher alkaline phosphatase levels at day 10 compared to day 7. At 14 and 21 days, modified SBAE supported higher proportions of red-dye-stained areas (calcium content).

Conclusion: Addition of a CaP coating to SBAE Ti by itself may affect key events of in vitro osteogenesis, ultimately resulting in enhanced matrix mineralization; additional P-15 functionalization has only limited synergistic effects. *J Periodontol 2013;84:1199-1210.*

KEY WORDS

Calcium phosphates; cells, cultured; collagen; osteoblasts; peptides; titanium.

* School of Dentistry of Ribeirão Preto, University of São Paulo, São Paulo, Brazil.
† Laboratory for the Study of Calcified Tissues and Biomaterials, University of Montréal, Montréal, QC.
‡ Institute of Material Science, Max Bergmann Center of Biomaterials, Dresden University of Technology, Dresden, Germany.
§ Faculty of Engineering, University of Ottawa, Ottawa, ON.

doi: 10.1902/jop.2012.120072

Various in vitro, in vivo, and clinical studies have reported enhanced bone repair around microstructured metal implants.[1-4] Novel strategies for implant surface modifications have been developed to further enhance and/or accelerate bone formation at the interface, particularly for areas of poor bone quality and for immediate loading applications.[5,6] These strategies include surface nanostructuring, modifications of surface chemistry and/or energy, and molecular functionalization.[7,8]

Enhanced biologic response (e.g., increased cell proliferation and cell activities, higher mRNA expression of osteoblast markers, and enhancement in matrix mineralization) has been reported as a consequence of the synergistic superimposition of submicron and/or nanoscale features on microtopographies.[9,10] Acid and/or alkaline treatments or coatings with calcium phosphate (CaP) phases have been exploited to alter the surface chemistry of metals, resulting in a promotion of interfacial apatite formation and osteoblast differentiation and activity.[11] In addition, the chemical modification of a hydrophobic microtopography yielded a highly hydrophilic surface that stimulates osteoblast functions and bone formation.[12,13]

Various approaches for biochemical surface modification rely on coating implant surfaces with the following: 1) major components of the bone extracellular matrix (ECM), i.e., hydroxyapatite and type I collagen;[14-18] 2) non-collagenous bone matrix proteins or growth factors;[7,19-21] and 3) peptides with known biologic activities.[22-25] Although various coatings with whole components of exogenous ECM induce beneficial cellular and tissue responses,[14,15,26,27] the lack of stability and immunogenicity of these molecules could limit their use.[28,29] In this context, surface functionalization with peptides is expected to advantageously stimulate the production of autogenous ECM by host cells. Type I collagen is the main structural protein in bone, and it promotes osteoblast cell adhesion and function.[30] Therefore, synthetic peptides mimicking amino acid sequences of collagen could be considered good candidates for surface functionalization for those applications in which faster and more stable bone integration is envisaged.[31] Here, we opted to use peptide 15 (P-15), a collagen-derived synthetic peptide analog of the cell-binding domain of type I collagen that has been demonstrated to promote osteogenic differentiation and enhance bone formation in various applications.[32-34]

The present study evaluates the effects of the functionalization of a microtopographic titanium (Ti) surface, created by sandblasting and acid etching (SBAE), on the development of the osteogenic phenotype in vitro. The surface was first coated with submicron-scale CaP as a strategy to functionalize with P-15. CaP coating was used for two reasons: 1) to increase the surface area and thus the amount of the adsorbed peptide; and 2) to mimic a native situation and thus limit any potential conformational changes of P-15.

MATERIALS AND METHODS

Ti Samples and Surface Characterization

Commercially pure Ti disks, 13 mm in diameter and 2 mm thick, were used in this study (total = 900 disks; n = 180 in each experimental group). The experimental groups for physicochemical characterization and biologic assays were classified according to the surface treatment: 1) machined; 2) SBAE; 3) SBAE with CaP coating (SBAE+CaP); 4) SBAE+CaP with a low concentration (20 μg/mL) of the synthetic peptide P-15 (P-low); and 5) SBAE+CaP with a high concentration (200 μg/mL) of P-15 (P-high). The machined Ti disks were purchased from a metal company,‖ whereas SBAE-based Ti disks were kindly provided by a dental company.¶ The detailed processes used to produce and sterilize such samples have not been disclosed by the manufacturer (proprietary processing).

The surface of the randomly selected machined and SBAE-based Ti was qualitatively and quantitatively evaluated in terms of topography and wettability. The sample imaging was performed using a field emission scanning electron microscope# (SEM) operated at 1.5 kV. In addition, the surface topography was visually and quantitatively characterized using an atomic force microscope** (AFM) in tapping mode at a scanning rate of 0.5 Hz and 512 acquisition points over an area of 1×1 μm. AFM images were analyzed with a software program†† to determine the root mean square (RMS) roughness. The surface wettability was assessed using the sessile drop method, as described previously.[35]

Cell Isolation and Culture of Osteogenic Cells

Primary osteogenic cells were isolated by sequential trypsin/collagenase digestion of calvarial bone from newborn Wistar rats.[36,37] All animal procedures were in accordance with the guidelines of the Animal Research Ethics Committee of the University of São Paulo (protocol 08.1.357.53.6). Cells were seeded on Ti disks placed in 24-well polystyrene plates‡‡ at a cell density of 2×10^4 cells per disk. The plated cells were cultured for periods of up to 21 days in α-minimum essential medium with L-glutamine§§

‖ Realum, São Paulo, São Paulo, Brazil.
¶ DENTSPLY Friadent, Mannheim, Germany.
# JEOL JSM-7400F, JEOL, Tokyo, Japan.
** JEOL JSPM-5200, JEOL.
†† WinSPM Data Processing Software, v.2.15, JEOL.
‡‡ Falcon, Franklin Lakes, NJ.
§§ Invitrogen, Carlsbad, CA.

supplemented with 10% fetal bovine serum,|||| 7 mM β-glycerophosphate,¶¶ 5 μg/mL ascorbic acid,## and 50 μg/mL gentamicin*** at 37°C in a humidified atmosphere with 5% carbon dioxide. The culture medium was changed every 3 days. Because of the inherent phenotypic heterogeneity of primary cultures, pre-osteoblastic MC3T3-E1 cells††† were selected for the evaluation of cell morphology by SEM.[38] The cells were plated on Ti disks at a cell density of 2×10^4 cells per disk and cultured for 3 days under the same conditions as those used for the primary cultures.

Cell Adhesion and Spreading and SEM Imaging of Cell Morphology

Cell adhesion and spreading were evaluated by direct fluorescence with green fluorescence dye-conjugated phalloidin,‡‡‡ which labels ubiquitous actin cytoskeleton, and 4′,6-diamidino-2-phenylindole, dihydrochloride§§§ for nuclear stain (for details, see *Immunolocalization of Bone ECM Proteins: Bone Sialoprotein and Osteopontin*). To assess cell adhesion and spreading,[38,39] the proportion of cells at stages 1 (round cells), 2 (round cells with filopodia), 3 (cells with cytoplasmic webbing), and 4 (well-flattened cells) was calculated from 100 adherent cells after 4 hours of culture for each surface, using randomly selected 10 to 15 microscopic fields (×40 objective). At day 3 of culture, MC3T3-E1 cells were processed for SEM imaging according to an established protocol.[36]

Cell Viability, Proportion of Proliferating Cells, and Total Cell Number

At days 1, 3, and 7 of culture, cell viability was evaluated by 3-[4,5-dimethylthiazol-2-yl]-2,5-diphenyltetrazolium bromide (MTT)|||||| assay. Briefly, cells were incubated with 100 μL MTT (5 mg/mL) in culture medium at 37°C for 4 hours. The medium was then aspirated from the well, and 1 mL acid-isopropanol (0.04N HCl in isopropanol) was added to each well. The plates were then stirred on a plate shaker for 5 minutes, and 200 μL of this solution was transferred to a 96-well format using opaque-walled transparent-bottomed plates.¶¶¶ The optical density was read at 570 nm on a plate reader,### and the data were expressed as absorbance.[40]

The proportion of proliferating cells at day 3 of culture was determined by double [(5S)-6-[4-[4-[4-[(2S)-6-azaniumyl-2-(4-butyltriazol-1-yl)hexanoyl] piperazin-1-yl]-6-[2-[2-(2-prop-2-ynoxyethoxy)ethoxy] ethylamino]-1,3,5-triazin-2-yl]piperazin-1-yl]-5-[4-(2-carboxyethyl)triazol-1-yl]-6-oxohexyl]azanium chloride (Ki-67)/4′,6′-diamidino-2-phenylindole (DAPI) labeling, as described previously.[41] The antibody used was rabbit polyclonal antihuman Ki-67**** (1:70). Briefly, the total number of DAPI-stained nuclei and Ki-67-expressing proliferating cells that were adherent on Ti disks was calculated by epifluorescence counting at ×40 objective. A minimum total of 200 cells were counted on three Ti disks for each group, and the data were expressed as percentage Ki-67-positive cells.

The blue dye exclusion assay was used to determine the total number of cells at day 7.[37] Briefly, cells were enzymatically detached from the Ti surfaces using 1 mM EDTA, 1.3 mg/mL collagenase, and 0.25% trypsin solution.†††† The total number of cells was counted after blue dye‡‡‡‡ staining using a hemocytometer. Cell adhesion was expressed as a percentage of the initial number of cells (2×10^4 cells per disk).

Immunolocalization of Bone ECM Proteins: Bone Sialoprotein and Osteopontin

At days 1, 3, 7, 10, and 14 of culture, cells were fixed for 10 minutes at room temperature using 4% paraformaldehyde in 0.1 M phosphate buffer (PB), pH 7.2. After washing in PB, they were processed for immunofluorescence labeling, as previously described in detail.[37] Primary monoclonal antibodies to bone sialoprotein (BSP)§§§§ (1:200) and osteopontin (OPN)||||||| (1:800) were used, followed by a mixture of red fluorescence-conjugated goat antimouse secondary antibody¶¶¶¶ (1:200) and green fluorescence-conjugated phalloidin#### (1:200). The cell nuclei were stained with 300 nM DAPI***** for 5 minutes After mounting with an antifade kit,††††† the samples were examined under epifluorescence using a light microscope‡‡‡‡‡ outfitted with a digital camera.§§§§§ A total area of ≈400 mm^2 (corresponding to three Ti disks) was examined for each labeling and time point. Representative digital images were processed with an image software program.||||||||

|||| Invitrogen.
¶¶ Sigma-Aldrich, St. Louis, MO.
Invitrogen.
*** Invitrogen.
††† ATCC CRL-2594, American Type Culture Collection, Manassas, VA.
‡‡‡ Alexa Fluor 488-conjugated phalloidin, Invitrogen.
§§§ DAPI, Invitrogen.
|||| Sigma-Aldrich.
¶¶¶ Thermo Fisher Scientific, Suwanee, GA.
μQuant, Bio-Tek Instruments, Winooski, VT.
**** DBS, Pleasanton, CA.
†††† Invitrogen.
‡‡‡‡ Trypan blue, Sigma-Aldrich.
§§§§ WVID1-9C5, Developmental Studies Hybridoma Bank, University of Iowa, Iowa City, IA.
|||||| MPIIIB10-1, Developmental Studies Hybridoma Bank, University of Iowa.
¶¶¶¶ Alexa Fluor 594-conjugated goat antimouse secondary antibody, Invitrogen.
Alexa Fluor 488-conjugated phalloidin, Invitrogen.
***** Invitrogen.
††††† Vectashield, Vector Laboratories, Burlingame, CA.
‡‡‡‡‡ Leica DMLB, Leica, Bensheim, Germany.
§§§§§ Leica DC 300F, Leica.
|||||||| Adobe Photoshop CS5.1 software, Adobe Systems, San Jose, CA.

Gene Expression Analysis: Real-Time Polymerase Chain Reaction

The gene expression of runt-related transcription factor 2 (RUNX2), alkaline phosphatase (ALP), BSP, and OPN was evaluated by real-time polymerase chain reaction (PCR) at days 7 and 10 of culture. The total RNA from cells was extracted using a total RNA isolation system kit¶¶¶¶¶ according to the instructions of the manufacturer. The concentration of RNA was determined by optical density at different wavelengths (260, 280, 230, and 320 nm) using a spectrophotometer.##### Complementary deoxyribonucleic acid (cDNA) was synthesized using 1 μg RNA through a reverse transcription reaction using a high-capacity cDNA reverse transcription kit****** according to the instructions of the manufacturer.

The reactions of real-time PCR were performed in a detection system†††††† using fluorogenic probes.‡‡‡‡‡‡ The standard PCR conditions were 50°C (2 minutes), 95°C (10 minutes), and 40 cycles of 95°C (15 seconds), 60°C (1 minute). For mRNA analysis, the relative level of gene expression was calculated in reference to GAPDH expression and normalized to the gene expression of cells cultured on machined surfaces (calibrator) using the cycle threshold method.[42]

ALP Activity

ALP activity was assayed at day 10 of culture through the release of thymolphthalein from thymolphthalein monophosphate using a commercial kit.§§§§§§37 The data were expressed as ALP activity normalized to total protein content, which was determined by a modified Lowry method.[41]

Proportion of Apoptotic Cells

At day 10 of culture, the proportion of apoptotic cells was determined by flow cytometry. Briefly, the cells were trypsinized and labeled with annexin V and propidium iodide (PI) using a commercial kit‖‖‖‖‖‖‖‖ according to the instructions of the manufacturer. The labeled cells were assayed on a flow cytometer¶¶¶¶¶¶ by acquiring 5,000 to 10,000 events and further analyzed by dot plot using specific software.###### The cells were quantified as follows: 1) annexin V negative/PI positive (viable cells); 2) annexin V positive/PI negative (cells in the initial stages of apoptosis); 3) annexin V positive/PI positive (cells in the advanced stages of apoptosis); and 4) annexin V negative/PI positive (necrotic cells).

Mineralized Bone-Like Nodule Formation

At days 14 and 21, the cultures were washed in Hanks' solution (Hanks' balanced salts supplemented with 0.35 g/L sodium bicarbonate*******), fixed in 70% ethanol at 4°C for 60 minutes, and washed in phosphate buffered saline and distilled water. The cultures were then stained with 2% red dye,††††††† pH 4.2, at room temperature for 15 minutes. Triple labeling red dye–BSP–DAPI was performed as described previously.[43] The images were obtained digitally by an epifluorescence microscope‡‡‡‡‡‡‡ and a high-resolution camera.§§§§§§§

Quantitative evaluation of mineralization was performed by red-dye extraction (calcium content) as described in detail previously.[44] To further characterize the mineralization process, Fourier transform infrared (FTIR) spectroscopy analysis was performed in red-dye-stained areas at day 14 of culture using an FTIR spectrometer‖‖‖‖‖‖‖‖ in reflectance mode. The spectra were obtained in the range of wave number from 4,000 to 400 cm^{-1} and signal averaged for 10 scans at a resolution of 4 cm^{-1}.

Statistical Analyses

Statistical analysis was performed using a parametric or non-parametric test, for independent data (analysis of variance [ANOVA] or Kruskal-Wallis test, respectively), followed by a multiple comparison test when applicable. The level of significance was 5%. The results are representative of experiments performed with at least two distinct primary cultures.

RESULTS

Surface topography and roughness at the nanometric level varied according to the surface treatment. CaP coating of SBAE surfaces reduced RMS values by ≈50%. However, additional functionalization with P-15 increased the nanoroughness (Figs. 1A and 1B; see Supplementary Table 1). High-resolution SEM analysis revealed that pristine and modified SBAE surfaces exhibited an inhomogeneous microtopography, whereas machined samples only showed micrometric and submicrometric traces of mechanical polishing (Fig. 2). In addition, all modified SBAE surfaces exhibited a submicron-scale needle-shaped coating, with needle-like structures ranging from 100 to 300 nm in length and with the maximum thickness of ≈40 nm. Interestingly, such structures were considerably less apparent for P-high (Figs. 2E, 2G, and 2I).

¶¶¶¶¶ SV Total RNA Isolation System Kit, Promega, Madison, WI.
GeneQuant 1300, GE Healthcare, Cardiff, UK.
****** High Capacity cDNA Reverse Transcription Kit, Applied Biosystems, Foster City, CA.
†††††† CFX96, Bio-Rad, Hercules, CA.
‡‡‡‡‡‡ TaqMan Probe System, Applied Biosystems, Carlsbad, CA.
§§§§§§ Labtest Diagnostica, Lagoa Santa, MG, Brazil.
‖‖‖‖‖‖‖‖ Apoptest-FITC Kit, Dako, Glostrup, Denmark.
¶¶¶¶¶¶ FACS Canto, BD Biosciences, San Jose, CA.
Diva v.6.0, BD Biosciences.
******* Sigma-Aldrich.
††††††† Alizarin Red S, Sigma-Aldrich.
‡‡‡‡‡‡‡ Leica DMLB, Leica.
§§§§§§§ Canon EOS Digital Rebel, 6.3 MP, EF100 f/2.8 macro lens, Canon, Lake Success, NY.
‖‖‖‖‖‖‖‖ PerkinElmer Spectrum GX, PerkinElmer Life and Analytical Sciences, Shelton, CT.

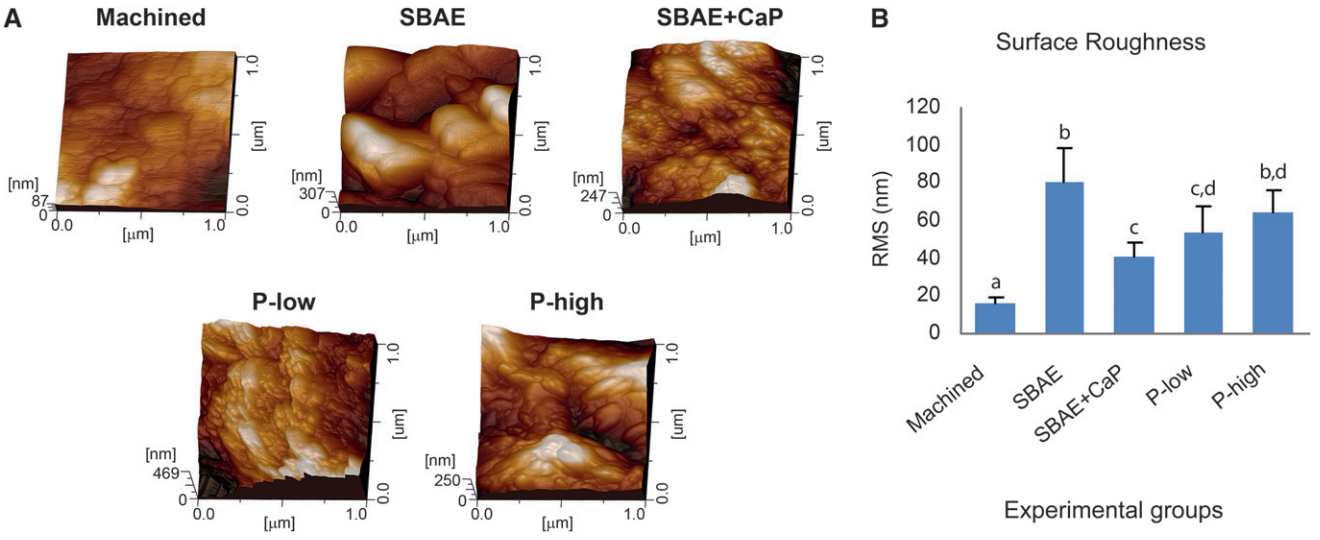

Figure 1.
*AFM topographies (1 × 1 μm^2) **(A)** and surface nanoroughness **(B)** (RMS) of machined, SBAE, and modified SBAE surfaces. Bars that share ≥1 letter are not significantly (P >0.05) different from each other.*

SEM imaging at 3 days of culture revealed that adherent cells on SBAE and modified SBAE surfaces were substantially less spread than those on the machined control. Although cells grown on machined Ti showed a direct contact between the whole cell body and the substrate, exhibiting short cytoplasmic processes, the cells on SBAE-based surfaces developed long cytoplasmic extensions of variable thickness, which established direct contact with either adjacent cells or the substrate (Figs. 2B, 2D, 2F, 2H, and 2J).

Statistically significant differences were observed among surfaces in terms of static contact angles (ANOVA, P <0.05). The mean values for the initial contact angle were ≈80° for machined surfaces and >100° for SBAE-based surfaces. Functionalization significantly reduced the contact angles at equilibrium to values of ≈40° (Fig. 3A; see Supplementary Table 2).

The assessment of cell adhesion and spreading at 4 hours revealed a significant reduction in the proportion of cells with a well-spread morphology (stages 3 and 4) on modified SBAE compared to machined Ti (Kruskal-Wallis test, P <0.05; Fig. 3B; see Supplementary Figure 1). In addition, significantly fewer cells were spread on P-high-functionalized surfaces compared to the SBAE control, whereas no differences among modified SBAE surfaces were observed (see Supplementary Table 3).

The MTT assay showed no significant differences among the groups at days 1, 3, and 7, except for significantly higher values in cultures grown on modified SBAE compared to SBAE at 3 days (Kruskal-Wallis test, P <0.05; Fig. 3C; see Supplementary Table 4). No differences in terms of cell proliferation were detected among the groups (ANOVA, P<0.05; see Supplementary Figs. 2 and 3). The total cell number was significantly lower (ANOVA, P <0.01) in cultures grown on SBAE-based surfaces at day 7 (see Supplementary Figure 4 and Supplementary Table 5).

For all surfaces, a significant proportion of cells exhibited OPN labeling in a perinuclear tubular network and in punctate deposits throughout the cytoplasm at 1 and 3 days of culture. Extracellular OPN labeling was only detected in cultures grown on modified SBAE, mostly adjacent to OPN-positive cells. Extracellular OPN labeling was more conspicuous at 3 days than at 1 day (Figs. 4A through 4J). At 7 and 10 days in all groups, BSP labeling was observed in the perinuclear region and in punctate deposits throughout the cytoplasm (data not shown). Extracellular BSP accumulation was detected in areas not necessarily associated with BSP-positive cells. Qualitatively, a reduced extracellular BSP labeling was observed in cultures grown on SBAE and SBAE+CaP, mainly at 7 days (Figs. 4K through 4T). At day 10, double labeling for BSP and OPN was evident in areas of cell multilayering only in the machined group (data not shown).

Real-time PCR analysis revealed that at day 7, the cells grown on SBAE-based surfaces exhibited significantly lower RUNX2 mRNA levels compared to the machined group (two-way ANOVA, P <0.05). A trend toward increased RUNX2 levels from 7 to 10 days was only observed for the modified SBAE groups (Fig. 5A; see Supplementary Table 6). The relative expression levels of ALP significantly

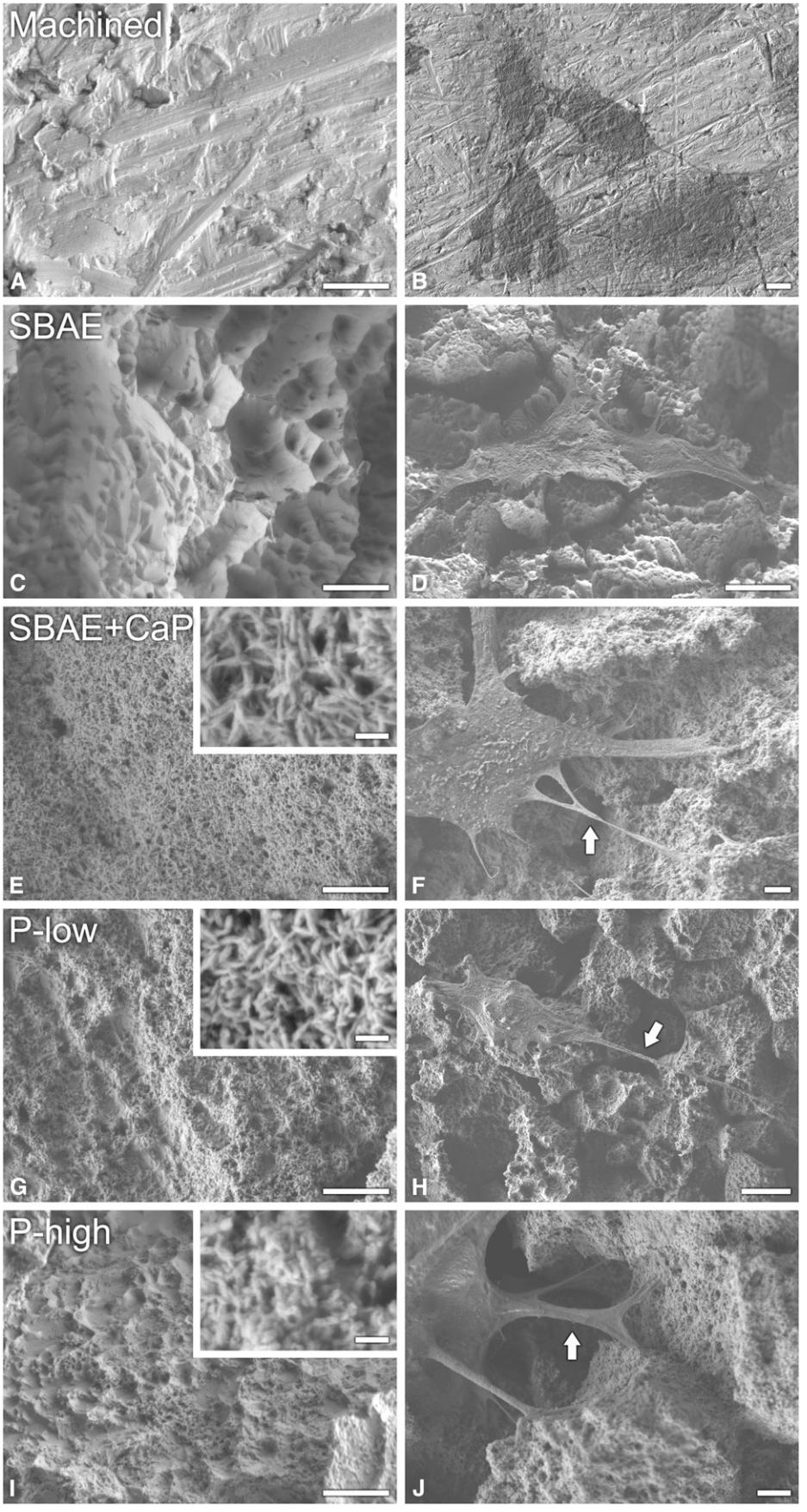

increased from 7 to 10 days in cultures grown on SBAE-based surfaces (two-way ANOVA, $P < 0.05$), whereas a significant reduction of ≈50% was detected in the machined group (Fig. 5A; see Supplementary Table 7). For all surfaces, BSP mRNA expression significantly increased from 7 to 10 days (two-way ANOVA, $P < 0.05$), with peak levels in cultures grown on the machined surface (Fig. 5A; see Supplementary Table 8). Significantly higher OPN mRNA levels were detected in cultures on SBAE-based surfaces at 7 days and on modified SBAE at 10 days, with peak levels for P-low (two-way ANOVA, $P < 0.05$) (Fig. 5A; see Supplementary Table 9).

After 10 days of culture, the cells grown on SBAE-based surfaces exhibited significantly lower ALP activity compared to the machined group (Kruskal-Wallis test, $P < 0.05$), whereas the functionalization with P-15 did not alter ALP activity (Fig. 5B; see Supplementary Table 10).

The apoptosis assay showed a trend toward the reduction in the proportion of cells in the initial phases of apoptosis (annexin V–positive/PI-negative cells) for cultures grown on the machined, P-low and P-high

Figure 2.
*High-resolution SEM imaging of machined, SBAE, and modified SBAE surfaces **(A, C, E, G,** and **I)** and of adherent MC3T3-E1 cells spread on Ti disks at 3 days **(B, D, F, H,** and **J)**. Modified SBAE surfaces exhibited a superficial layer of submicron-scale needle-shaped material (insets in E, G, and I), which was less apparent for P-high. Adherent cells on SBAE and modified SBAE were substantially less spread than the cells on the machined group, showing long cytoplasmic extensions that interacted with other cells and the substrate (F, H, and J, arrows). Scale bars: A, C, E, F, G, I, and J = 2 μm; B, D, and H = 10 μm; insets in E, G, and I = 200 nm.*

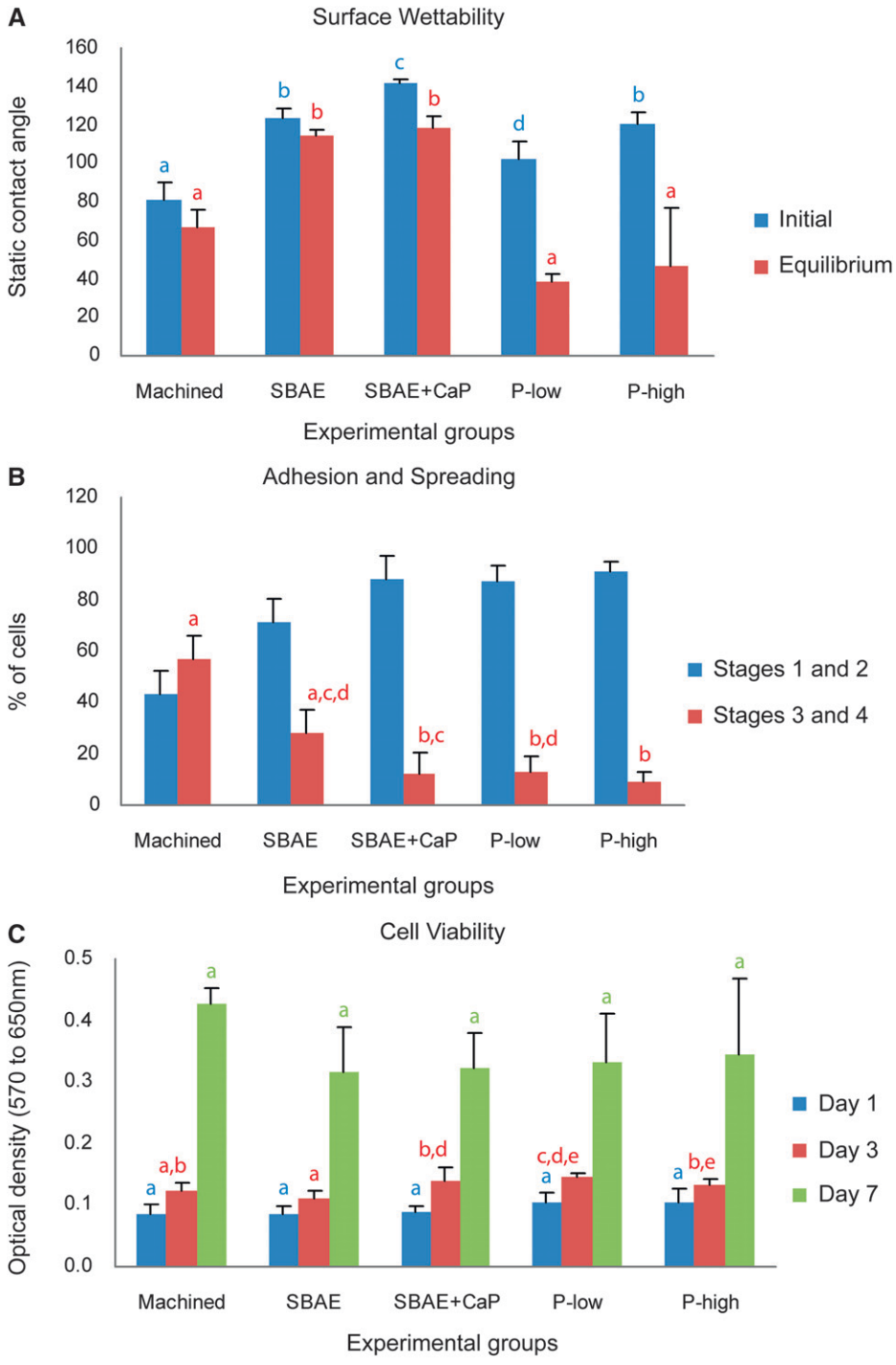

Figure 3.
A) *Surface wettability analysis by means of the sessile drop method using a drop of the cell culture medium on each surface.* ***B)*** *Proportion of osteogenic cells (100 cell count, ×40 objective) at different stages of adhesion and spreading on machined, SBAE, and modified SBAE surfaces at 4 hours.* ***C)*** *Cell viability (MTT, optical density) of osteogenic cell cultures grown on machined, SBAE, and modified SBAE surfaces at days 1, 3, and 7. Bars that share ≥1 letter of the same color are not significantly (P >0.05) different from each other.*

surfaces; at the same time, P-low and P-high doubled the proportion of cells in the advanced stages of apoptosis (annexin V–positive/PI-positive cells) compared to cultures on SBAE and machined Ti (see Supplementary Figure 5 and Supplementary Table 11).

A significant enhancement in matrix mineralization at 14 and 21 days of culture was observed in cultures on modified SBAE compared to the SBAE and machined groups (two-way ANOVA, P <0.05; Fig. 5C; see Supplementary Table 12). A significant increase from 14 to 21 days of culture was detected only in the P-low cultures. Although no major differences were noticed among the modified SBAE at day 14, the red-dye values were significantly higher for P-low compared to P-high at day 21. Using the same culture conditions with no cells, minimal red-dye values were detected at day 14 in all surfaces, including those coated with CaP (Fig. 5C).

Morphologically, typical mineralized nodules, brownish/reddish in color, were observed in cultures grown on the machined group at days 14 and 21 of culture. However, for SBAE-based surfaces, such structures were only occasionally detected at day 14 and were more frequent at day 21, although in a lesser quantity than cultures grown on the machined control (Fig. 6). Diffuse red-dye-stained areas, which were reddish for cultures on machined

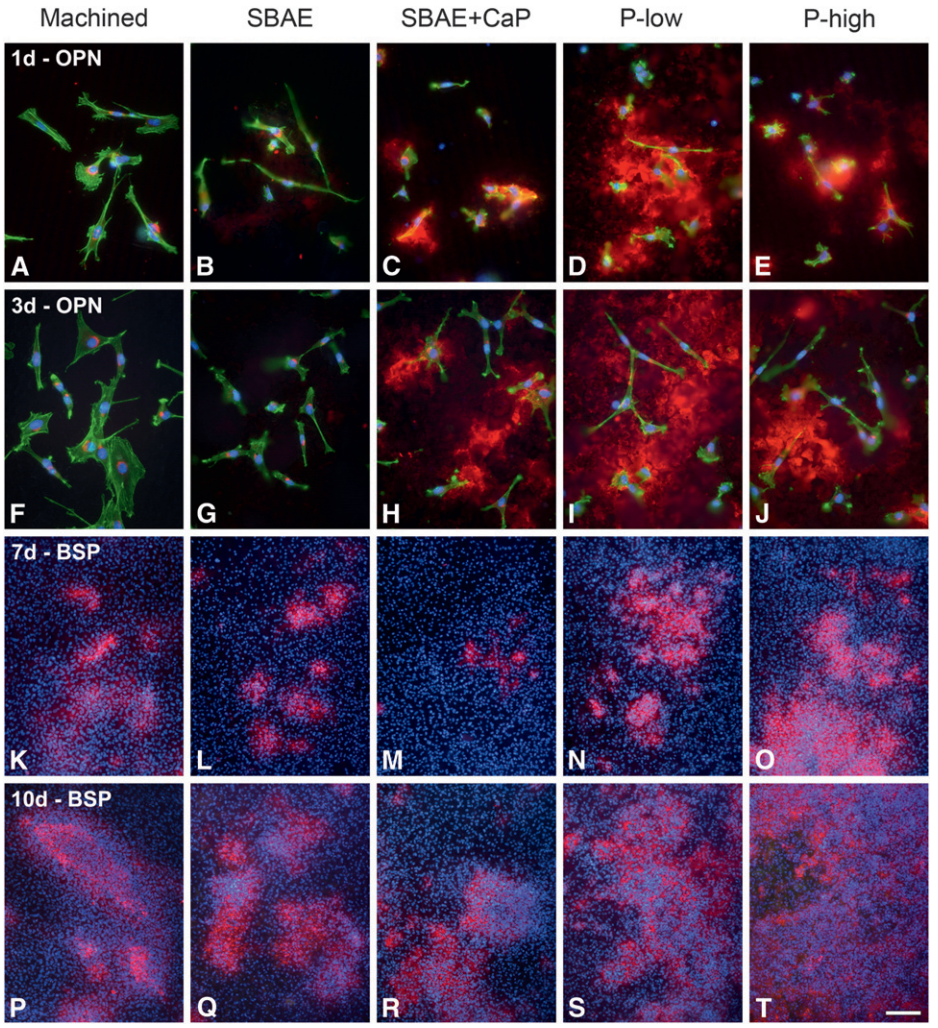

Figure 4.
Epifluorescence of osteogenic cell cultures grown on machined, SBAE, and modified SBAE surfaces at 1 ***(A through E)****, 3* ***(F through J)****, 7* ***(K through O)****, and 10* ***(P through T)*** *days. Red indicates OPN (A through J) and BSP (K through T) labeling, green indicates actin cytoskeleton (A through J), and blue indicates cell nuclei (A through T). Extracellular OPN labeling is abundant and prominent in cultures grown on SBAE+CaP, P-low, and P-high (C through E and H through J). Large BSP-positive areas are clearly observed in P-low and P-high at 10 days (S and T). Scale bar: A through J = 50 μm; K through T = 200 μm. d = day(s).*

surfaces and brownish for the ones on SBAE and modified SBAE, were also observed at both time points (Figs. 6A through 6J). Epifluorescence revealed red-dye-stained nodules exhibiting an irregular contour (Figs. 6K through 6T) and labeling for BSP, which was remarkably weaker for cultures on SBAE-based surfaces (compare Figs. 6L through 6O to Fig. 6K). FTIR analysis of red-dye-stained areas revealed vibrational bands from 900 to 1,200 cm^{-1} (phosphate/mineral) and from 1,580 to 1,720 cm^{-1} (amide I/organic matrix) in all groups, with more pronounced peaks for the machined group (see Supplementary Figure 6).

The numerical data are summarized in Supplementary Table 13.

DISCUSSION

This in vitro study demonstrates that coating of an SBAE Ti microtopography with submicron-scale CaP by itself may affect key parameters of the progression of the osteogenic phenotype. A reduction in the proportion of spread cells and a higher accumulation of extracellular OPN at early time points were observed for cultures grown on modified SBAE surfaces. In addition, changes in the mRNA profile of osteogenic markers at 7 and 10 days of culture preceded the occurrence of significantly larger areas of calcified matrix at days 14 and 21 for modified SBAE compared to controls. Functionalization with P-15 promoted only limited synergistic effects.

CaP-based coatings on Ti have been shown to promote biocompatibility and osseointegration, depending on the type of coating.[45] In the present study, a submicron-scale CaP coating comparable with that developed by Rössler et al.[46] is deposited on SBAE Ti to achieve the loading of P-15 at two concentrations. During the first 10 days of culture, the modified SBAE surfaces promoted a reduction in cell spreading, cell number, the occurrence of larger extracellular OPN deposits, and a trend toward a higher proportion of cells at advanced stages of apoptosis. Although these findings could suggest an earlier acquisition of a more mature osteoblastic phenotype,[23,30] the higher MTT values together with lower osteoblast marker mRNA levels and ALP activity suggest the occurrence of a transient delay in osteogenic differentiation accompanied by changes in cell proliferation dynamics (although not detected at day 3 by Ki-67) and the rate of apoptosis. Such findings are likely attributable, at least in part, to the interaction of cells with the increased surface area provided by the CaP coating, a common feature for the modified SBAE. A similar osteogenic cell response has been observed for porous Ti.[47] Importantly, the possibility

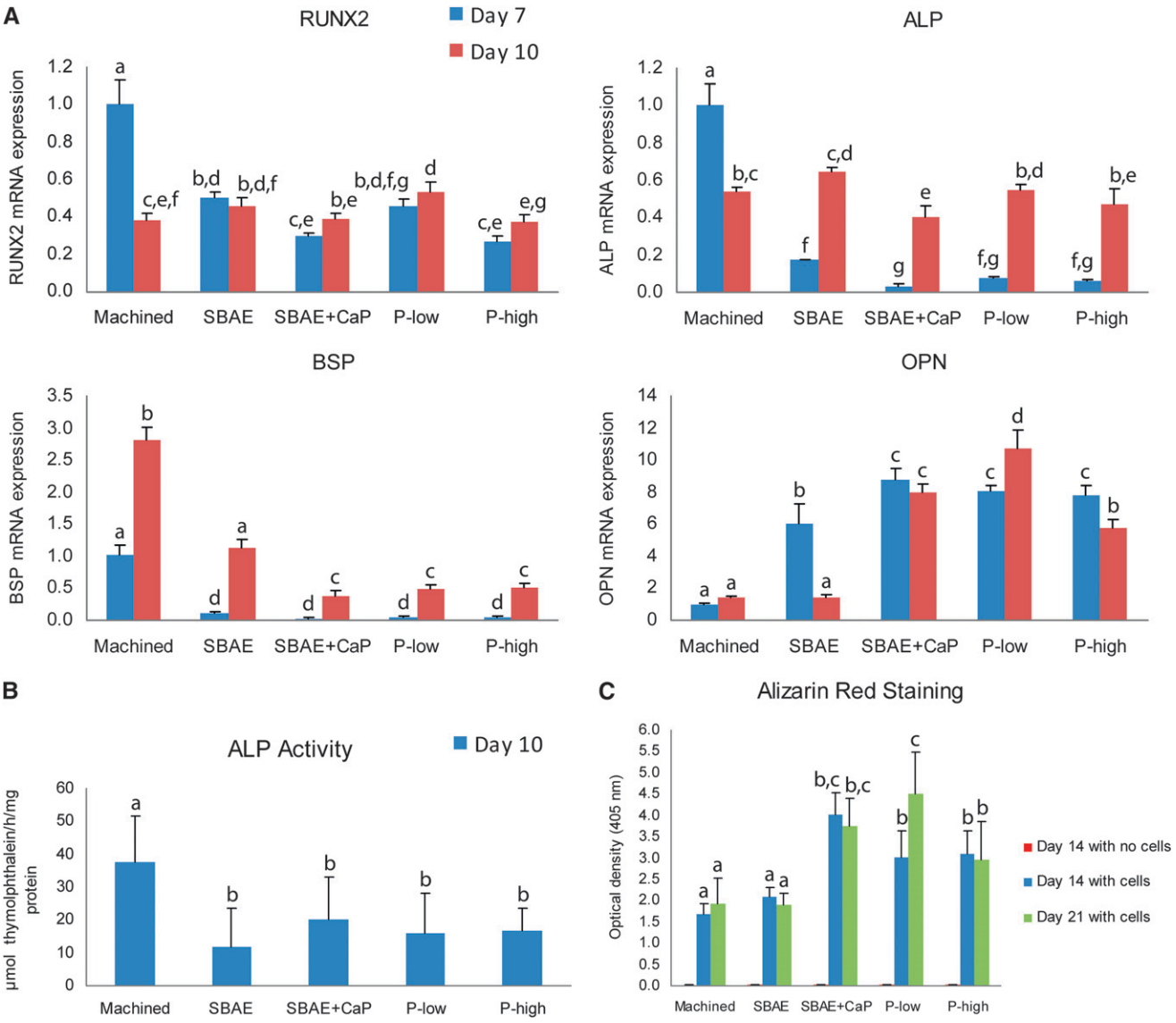

Figure 5.

A) *Relative mRNA expression of RUNX2, ALP, BSP, and OPN levels in osteogenic cell cultures grown on machined, SBAE, and modified SBAE surfaces at days 7 and 10. The data were normalized to GAPDH mRNA levels, and value 1 was attributed to cultures grown on machined surfaces at day 7.* ***B)*** *ALP activity (micromolar thymolphthalein per hours per milligrams protein) of osteogenic cell cultures grown on machined, SBAE, and modified SBAE surfaces at day 10.* ***C)*** *Quantitative analysis of red-dye-stained osteogenic cultures grown on machined, SBAE, and modified SBAE surfaces at days 14 and 21. Notice the higher values of red dye in the modified SBAE cultures. Bars that share ≥1 letter are not significantly (P >0.05) different from each other.*

that early enhanced extracellular OPN labeling takes place because of an enhanced adsorption of the protein on the CaP coating, and not because of a higher osteoblastic activity, should not be ruled out and must be further investigated.

At 14 and 21 days of culture, modified SBAE supported the occurrence of significantly larger areas of mineralized ECM, mostly in a diffuse, non-nodular pattern. The physiologic-like nature of the mineral deposits associated with a collagen-based organic matrix was demonstrated by FTIR analysis.[48] Interestingly, the formation of woven bone-like nodules, typically observed in cultures grown on machined Ti,[37] was delayed and clearly less prominent in cultures grown on modified SBAE. This could suggest that terminal osteoblastic differentiation on modified SBAE (and also on SBAE) would not necessarily depend on the cell multilayering that takes place after confluence on flat, dense substrates and precedes and colocalizes with nodule formation in calvarial cell cultures, a finding that has also been demonstrated for other microtopographies.[49] Despite a trend toward the use of hierarchically structured implants, the higher bone marker gene

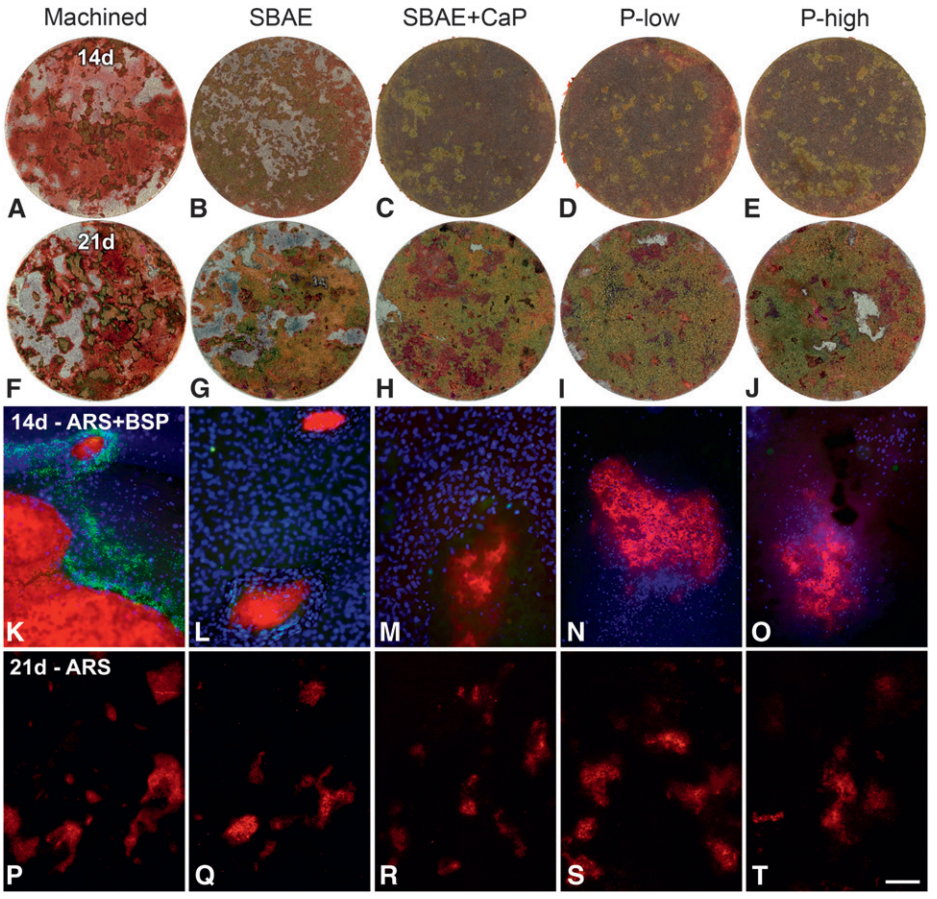

Figure 6.
*Macroscopic **(A through J)** and microscopic **(K through T)** imaging of osteogenic cell cultures on machined, SBAE, and modified SBAE surfaces at days 14 (A through E and K through O) and 21 (F through J and P through T). The cultures were stained with red dye to detect calcium deposits (K through T). Red fluorescence indicates red-dye-stained nodules (K through O). Green fluorescence indicates BSP labeling, whereas blue fluorescence indicates cell nuclei. Scale bar: A through J = 2.8 mm; K through M = 100 μm; N and O = 200 μm; P through T = 800 μm. d = days; ARS = Alizarin Red S.*

expression observed on machined Ti, together with the earlier mineralized nodule formation on machined Ti compared to modified SBAE in our in vitro conditions, support the idea that machined surfaces would also benefit from CaP coatings.

Functionalization with the two peptide concentrations used significantly changed the contact angles at equilibrium, transforming the highly hydrophobic SBAE+CaP into a moderately hydrophilic surface. Hydrophilic Ti surfaces have been shown to promote the enhancement of mineralized ECM formation in vitro[37] and to accelerate osseointegration.[12,13] In this context, although changes in wettability could contribute to the higher osteogenic potential for cultures grown on P-low at day 21, it would not account for the differences noticed between P-low and P-high, which exhibited the same contact angle. In an in vivo model using grit-blasted and acid-etched dental implants functionalized with P-15,[25] significantly higher bone-to-implant contact rates were achieved with the high concentration of P-15; however, both concentrations of the peptide (20 and 200 μg/mL) showed increased peri-implant bone density compared to the control. Because no CaP-coated Ti with no peptide was used in that study, the positive effects on osseointegration would not necessarily be attributable to the P-15 functionalization. Importantly, a more recent study from the same group,[50] with proper controls, revealed no significant impact of P-15 on interfacial bone formation at concentrations ranging from 20 to 400 μg/mL.

CONCLUSIONS

The present in vitro results demonstrated that the strategy used to functionalize SBAE Ti microtopography might affect key parameters of the progression of the osteogenic phenotype. Despite the occurrence of earlier osteoblastic cell spreading and differentiation for the machined Ti, the SBAE+CaP, P-low, and P-high surfaces all equally supported changes in the mRNA expression profile of key osteoblast markers, ultimately resulting in enhanced ECM mineralization. However, only limited synergistic effects were achieved with the P-15 functionalization.

ACKNOWLEDGMENTS

This study was supported by State of São Paulo Research Foundation Grant 2008/54027-9 and the National Council of Scientific and Technological Development. AN acknowledges support from Canadian Institutes of Health Research and Natural Sciences and Engineering Research Council of Canada. KKYP was the recipient of a master's fellowship from The Coordination for the Improvement of Higher Education Personnel, Brasília, DF, Brazil. OCA was the recipient of an internship scholarship from the State of São Paulo Research Foundation. The MPIIIB10-1 and WVID1-9C5 antibodies,

developed by M. Solursh and A. Franzen, University of Iowa, Iowa City, Iowa, were obtained from the Developmental Studies Hybridoma Bank (University of Iowa, Iowa City, Iowa). The authors thank Roger R. Fernandes and Larissa M.S. de Castro-Raucci (University of São Paulo, Ribeirão Preto, São Paulo, Brazil) for their technical assistance; Murilo Crovace (Federal University of São Carlos, São Carlos, São Paulo, Brazil) for the FTIR analysis; and Sylvia Zalzal (University of Montréal, Montréal, Quebec) for the SEM imaging. Drs. Scharnweber and Wolf-Brandstetter report financial support from DENTSPLY Friadent, Mannheim, Germany for the development of the coating process. Drs. Pereira, Alves, Novaes Jr., F.S. de Oliveira, Yi, Zaniquelli, Variola, Nanci, Rosa, and P.T. de Oliveira report no conflicts of interest related to this study.

REFERENCES

1. Matsuzaka K, Walboomers XF, Yoshinari M, Inoue T, Jansen JA. The attachment and growth behavior of osteoblast-like cells on microtextured surfaces. *Biomaterials* 2003;24:2711-2719.
2. Schwartz Fo HO, Novaes AB Jr., de Castro LMS, Rosa AL, de Oliveira PT. In vitro osteogenesis on a microstructured titanium surface with additional submicron-scale topography. *Clin Oral Implants Res* 2007;18: 333-344.
3. Mendonça G, Mendonça DB, Aragão FJ, Cooper LF. Advancing dental implant surface technology—From micron- to nanotopography. *Biomaterials* 2008;29: 3822-3835.
4. Schwarz F, Wieland M, Schwartz Z, et al. Potential of chemically modified hydrophilic surface characteristics to support tissue integration of titanium dental implants. *J Biomed Mater Res B Appl Biomater* 2009; 88:544-557.
5. Bornstein MM, Cionca N, Mombelli A. Systemic conditions and treatments as risks for implant therapy. *Int J Oral Maxillofac Implants* 2009;24(Suppl.):12-27.
6. Beutner R, Michael J, Schwenzer B, Scharnweber D. Biological nano-functionalization of titanium-based biomaterial surfaces: A flexible toolbox. *J R Soc Interface* 2010;7(Suppl. 1):S93-S105.
7. Junker R, Dimakis A, Thoneick M, Jansen JA. Effects of implant surface coatings and composition on bone integration: A systematic review. *Clin Oral Implants Res* 2009;20(Suppl. 4):185-206.
8. Variola F, Brunski JB, Orsini G, Tambasco de Oliveira P, Wazen R, Nanci A. Nanoscale surface modifications of medically relevant metals: State-of-the art and perspectives. *Nanoscale* 2011;3:335-353.
9. Mendonça G, Mendonça DB, Aragão FJ, Cooper LF. The combination of micron and nanotopography by H(2)SO(4)/H(2)O(2) treatment and its effects on osteoblast-specific gene expression of hMSCs. *J Biomed Mater Res A* 2010;94:169-179.
10. Wieland M, Textor M, Chehroudi B, Brunette DM. Synergistic interaction of topographic features in the production of bone-like nodules on Ti surfaces by rat osteoblasts. *Biomaterials* 2005;26:1119-1130.
11. Kizuki T, Takadama H, Matsushita T, Nakamura T, Kokubo T. Preparation of bioactive Ti metal surface enriched with calcium ions by chemical treatment. *Acta Biomater* 2010;6:2836-2842.
12. Buser D, Broggini N, Wieland M, et al. Enhanced bone apposition to a chemically modified SLA titanium surface. *J Dent Res* 2004;83:529-533.
13. Zhao G, Schwartz Z, Wieland M, et al. High surface energy enhances cell response to titanium substrate microstructure. *J Biomed Mater Res A* 2005;74:49-58.
14. Morra M, Cassinelli C, Cascardo G, et al. Surface engineering of titanium by collagen immobilization. Surface characterization and in vitro and in vivo studies. *Biomaterials* 2003;24:4639-4654.
15. Rammelt S, Schulze E, Bernhardt R, et al. Coating of titanium implants with type-I collagen. *J Orthop Res* 2004;22:1025-1034.
16. Morra M, Cassinelli C, Cascardo G, et al. Collagen I-coated titanium surfaces: Mesenchymal cell adhesion and in vivo evaluation in trabecular bone implants. *J Biomed Mater Res A* 2006;78:449-458.
17. Meirelles L, Arvidsson A, Andersson M, Kjellin P, Albrektsson T, Wennerberg A. Nano hydroxyapatite structures influence early bone formation. *J Biomed Mater Res A* 2008;87:299-307.
18. Yang GL, He FM, Hu JA, Wang XX, Zhao SF. Biomechanical comparison of biomimetically and electrochemically deposited hydroxyapatite-coated porous titanium implants. *J Oral Maxillofac Surg* 2010;68: 420-427.
19. Wikesjö UM, Huang YH, Xiropaidis AV, et al. Bone formation at recombinant human bone morphogenetic protein-2-coated titanium implants in the posterior maxilla (Type IV bone) in non-human primates. *J Clin Periodontol* 2008;35:992-1000.
20. Schouten C, Meijer GJ, van den Beucken JJ, Spauwen PH, Jansen JA. Effects of implant geometry, surface properties, and TGF-beta1 on peri-implant bone response: An experimental study in goats. *Clin Oral Implants Res* 2009;20:421-429.
21. Susin C, Qahash M, Polimeni G, et al. Alveolar ridge augmentation using implants coated with recombinant human bone morphogenetic protein-7 (rhBMP-7/rhOP-1): Histological observations. *J Clin Periodontol* 2010;37:574-581.
22. Roessler S, Born R, Scharnweber D, Worch H, Sewing A, Dard M. Biomimetic coatings functionalized with adhesion peptides for dental implants. *J Mater Sci Mater Med* 2001;12:871-877.
23. Tosatti S, Schwartz Z, Campbell C, et al. RGD-containing peptide GCRGYGRGDSPG reduces enhancement of osteoblast differentiation by poly(L-lysine)-graft-poly (ethylene glycol)-coated titanium surfaces. *J Biomed Mater Res A* 2004;68:458-472.
24. García AJ, Reyes CD. Bio-adhesive surfaces to promote osteoblast differentiation and bone formation. *J Dent Res* 2005;84:407-413.
25. Lutz R, Srour S, Nonhoff J, Weisel T, Damien CJ, Schlegel KA. Biofunctionalization of titanium implants with a biomimetic active peptide (P-15) promotes early osseointegration. *Clin Oral Implants Res* 2010;21:726-734.
26. Geissler U, Hempel U, Wolf C, Scharnweber D, Worch H, Wenzel K. Collagen type I-coating of Ti6Al4V promotes adhesion of osteoblasts. *J Biomed Mater Res* 2000;51:752-760.

27. de Assis AF, Beloti MM, Crippa GE, de Oliveira PT, Morra M, Rosa AL. Development of the osteoblastic phenotype in human alveolar bone-derived cells grown on a collagen type I-coated titanium surface. *Clin Oral Implants Res* 2009;20:240-246.
28. Lynn AK, Yannas IV, Bonfield W. Antigenicity and immunogenicity of collagen. *J Biomed Mater Res B Appl Biomater* 2004;71:343-354.
29. Liu W, Merrett K, Griffith M, et al. Recombinant human collagen for tissue engineered corneal substitutes. *Biomaterials* 2008;29:1147-1158.
30. Lynch MP, Stein JL, Stein GS, Lian JB. The influence of type I collagen on the development and maintenance of the osteoblast phenotype in primary and passaged rat calvarial osteoblasts: Modification of expression of genes supporting cell growth, adhesion, and extracellular matrix mineralization. *Exp Cell Res* 1995;216:35-45.
31. Shekaran A, García AJ. Extracellular matrix-mimetic adhesive biomaterials for bone repair. *J Biomed Mater Res A* 2011;96:261-272.
32. Bhatnagar RS, Qian JJ, Wedrychowska A, Sadeghi M, Wu YM, Smith N. Design of biomimetic habitats for tissue engineering with P-15, a synthetic peptide analogue of collagen. *Tissue Eng* 1999;5:53-65.
33. Yang XB, Bhatnagar RS, Li S, Oreffo RO. Biomimetic collagen scaffolds for human bone cell growth and differentiation. *Tissue Eng* 2004;10:1148-1159.
34. Gomar F, Orozco R, Villar JL, Arrizabalaga F. P-15 small peptide bone graft substitute in the treatment of non-unions and delayed union. A pilot clinical trial. *Int Orthop* 2007;31:93-99.
35. Adamson AW, Gast AP. The solid–liquid interface-contact angle. In: Adamson AW, Gast AP, eds. *Physical Chemistry of Surfaces*. New York: John Wiley & Sons; 1997:347-389.
36. de Oliveira PT, Nanci A. Nanotexturing of titanium-based surfaces upregulates expression of bone sialoprotein and osteopontin by cultured osteogenic cells. *Biomaterials* 2004;25:403-413.
37. de Oliveira PT, Zalzal SF, Beloti MM, Rosa AL, Nanci A. Enhancement of in vitro osteogenesis on titanium by chemically produced nanotopography. *J Biomed Mater Res A* 2007;80:554-564.
38. Vetrone F, Variola F, Tambasco de Oliveira P, et al. Nanoscale oxidative patterning of metallic surfaces to modulate cell activity and fate. *Nano Lett* 2009;9:659-665.
39. Rajaraman R, Rounds DE, Yen SP, Rembaum A. A scanning electron microscope study of cell adhesion and spreading in vitro. *Exp Cell Res* 1974;88:327-339.
40. Mosmann T. Rapid colorimetric assay for cellular growth and survival: Application to proliferation and cytotoxicity assays. *J Immunol Methods* 1983;65:55-63.
41. de Oliva MA, Maximiano WM, de Castro LM, et al. Treatment with a growth factor-protein mixture inhibits formation of mineralized nodules in osteogenic cell cultures grown on titanium. *J Histochem Cytochem* 2009;57:265-276.
42. Livak KJ, Schmittgen TD. Analysis of relative gene expression data using real-time quantitative PCR and the 2(-Delta Delta C(T)) Method. *Methods* 2001;25:402-408.
43. da Silva RA, Leonardo MR, da Silva LA, de Castro LM, Rosa AL, de Oliveira PT. Effects of the association between a calcium hydroxide paste and 0.4% chlorhexidine on the development of the osteogenic phenotype in vitro. *J Endod* 2008;34:1485-1489.
44. Gregory CA, Gunn WG, Peister A, Prockop DJ. An Alizarin red-based assay of mineralization by adherent cells in culture: Comparison with cetylpyridinium chloride extraction. *Anal Biochem* 2004;329:77-84.
45. Narayanan R, Seshadri SK, Kwon TY, Kim KH. Calcium phosphate-based coatings on titanium and its alloys. *J Biomed Mater Res B Appl Biomater* 2008;85:279-299.
46. Rössler S, Sewing A, Stölzel M, et al. Electrochemically assisted deposition of thin calcium phosphate coatings at near-physiological pH and temperature. *J Biomed Mater Res A* 2003;64:655-663.
47. Rosa AL, Crippa GE, de Oliveira PT, Taba M Jr., Lefebvre LP, Beloti MM. Human alveolar bone cell proliferation, expression of osteoblastic phenotype, and matrix mineralization on porous titanium produced by powder metallurgy. *Clin Oral Implants Res* 2009;20:472-481.
48. Boyan BD, Bonewald LF, Paschalis EP, et al. Osteoblast-mediated mineral deposition in culture is dependent on surface microtopography. *Calcif Tissue Int* 2002;71:519-529.
49. Kirmizidis G, Birch MA. Microfabricated grooved substrates influence cell-cell communication and osteoblast differentiation in vitro. *Tissue Eng Part A* 2009;15:1427-1436.
50. Lutz R, Prechtl C, Nonhoff J, Weisel T, Damien CJ, Schlegel KA. Biofunctionalization of the implant surface with different concentrations of a synthetic peptide (P-15). *Clin Oral Implants Res* 2013;24:781-786.

Correspondence: Dr. Paulo Tambasco de Oliveira, Department of Morphology, University of São Paulo, School of Dentistry of Ribeirão Preto, Av. do Café, s/n, 14040-904, Ribeirão Preto, São Paulo, Brazil. Fax: 55-16-3633-0999; e-mail: tambasco@usp.br.

Submitted January 29, 2012; accepted for publication September 10, 2012.